High Level QM/MM Modeling of the Formation of the Tetrahedral Intermediate in the Acylation of Wild Type and K73A Mutant TEM-1 Class A β-Lactamase[†]

Johannes C. Hermann,[‡,§,||] Juliette Pradon,[‡] Jeremy N. Harvey,*[,‡] and Adrian J. Mulholland*[,‡]

Centre for Computational Chemistry, School of Chemistry, University of Bristol, Bristol BS8 1TS, U.K., and Roche Palo Alto LLC, 3431 Hillview Ave, Palo Alto, California 94304

Received: April 22, 2009; Revised Manuscript Received: September 15, 2009

The breakdown of β-lactam antibiotics by β-lactamases is the most important resistance mechanism of Gram negative bacteria against these drugs. The reaction mechanism of class A β-lactamases, the most widespread family of these enzymes, consists of two main steps: acylation of an active site serine by the antibiotic, followed by deacylation and release of the cleaved compound. We have investigated the first step in acylation (the formation of the tetrahedral intermediate) for the reaction of benzylpenicillin in the TEM-1 enzyme using high level combined quantum mechanics/molecular mechanics (QM/MM) methods. Structures were optimized at the B3LYP/6-31+G(d)/CHARMM27 level, with energies for key points calculated up to the ab initio SCS-MP2/aug-cc-pVTZ/CHARMM27 level. The results support a mechanism in which Glu166 removes a proton (via an intervening water molecule) from Ser70, which in turn attacks the β-lactam of the antibiotic. Depending on the method used, the calculated barriers range from 3 to 12 kcal mol^{-1} for this step, consistent with experimental data. We have also modeled this reaction step in a model of the K73A mutant enzyme. The barrier to reaction in this mutant model is found to be slightly higher: the results indicate that Lys73 stabilizes the transition state, in particular deprotonated Ser70, lowering the barrier by about 1.7 kcal mol^{-1}. This finding may help to explain the conservation of Lys73, in addition to the role we have previously found for it in the later stages of the reaction (Hermann et al. *Org. Biomol. Chem.* **2006**, *4*, 206−210).

Introduction

β-Lactamases are a primary cause of bacterial resistance to β-lactam antibiotics for many important human pathogens (particularly Gram negative bacteria).[1] The labile and reactive β-lactam bond of these antibacterial drugs is vital for their antibiotic effect, because it acylates an active site serine of a penicillin binding protein (PBP).[2] PBPs are bacterial enzymes responsible for building and maintaining the murein part of the bacterial cell wall.[3] Acylation of the active site serine by β-lactam-antibiotics leads to inhibition of PBPs and to nonfunctional, unstable cell walls and bacterial cell death.[4] β-Lactamases cleave the antibiotic β-lactam bond very efficiently and release the products, which have lost all antibiotic potency. β-Lactamases and especially the most widespread family, the class A β-lactamases,[5] are present in almost every pathogenic bacterial strain and pose a serious and growing threat to antibacterial therapy, and therefore to human health and quality of life.[6−11] Detailed knowledge about the reaction at a molecular level should reveal important interactions and stabilization mechanisms and help develop urgently needed new antibiotics that are less susceptible to β-lactamase hydrolysis, and better inhibitors than those currently used clinically such as clavulanate.[12]

The reaction mechanism of class A β-lactamases consists of two main steps: in the first step (acylation), the active site serine (Ser70[13]) is acylated. In the second step (deacylation), the ester of the acylenzyme is hydrolyzed, returning the active site to its original state. The proposed mechanism for the deacylation step is widely accepted and is supported by a number of experiments and a recent modeling study.[14−17] In the deacylation process, Glu166 acts as a base to deprotonate a structurally conserved water molecule for nucleophilic attack on the acyl-enzyme intermediate.

The mechanism of the acylation step is more controversial, with a number of proposals put forward.[15,18−22] A central question is which residue acts as the general base and activates Ser70 for nucleophilic attack on the β-lactam bond. Either Lys73 (if it were neutral), or Glu166 via an intervening water molecule, would be in an excellent position to abstract a proton from Ser70 and are therefore the most likely candidates for acting as the general base.[15,23−25] This abstraction could happen by direct, concerted proton transfers or—as recently proposed—in a mechanism involving both residues, Lys73 and Glu166.[26] Examples of lysine acting as a base in enzymes (e.g., in fatty acid amide hydrolase[27]) are known, but to perform this function efficiently, the p*K*a of its side chain must be lowered significantly. Other hypotheses for the acylation mechanism involve the carboxylate functional group, which every β-lactam antibiotic contains, as the base in the acylation.[28]

Class A β-lactamases show decreased acylation rates when Lys73 or Glu166 is replaced by site-directed mutagenesis, strengthening theories that one of these two residues acts as the general base.[16,24,29−31] A number of experimental and theoretical investigations have been conducted that either favor Glu166 as the base, initiating reaction, or propose Lys73 to be neutral and to act as the base by directly abstracting a proton from Ser70.[26,32−41] According to the mechanism involving Glu166, its carboxylate group activates Ser70 through a hydrogen bond network, where the proton of Ser70 is transferred to an intervening water molecule, which in turn protonates

[†] Part of the "Walter Thiel Festschrift".
[‡] University of Bristol.
[§] Roche Palo Alto LLC.
[||] Current address: Roche Nutley, 340 Kingsland St, Nutley, New Jersey 07110.

10.1021/jp9037254 CCC: $40.75
Published on Web 09/30/2009

SCHEME 1: Key Processes of the Acylation Mechanism Modeled Here for Formation of the Tetrahedral Intermediate (TI) from the Michaelis (Enzyme−Substrate) Complex (MC) in the TEM-1 Class A β-Lactamase[a]

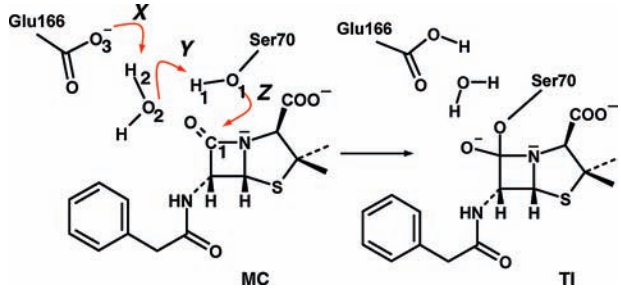

[a] The modeled processes are labeled X, Y, and Z.

Glu166 (see Scheme 1). We have previously modeled this mechanism of the full acylation reaction with a semiempirical (AM1/CHARMM22) QM/MM method with energy corrections at the B3LYP/6-31+G(d) level: the calculated (corrected) reaction energetics were consistent with experimental data (e.g., kinetics of the overall reaction and crystal structures).[37,38,42−44] Higher-level energy corrections were found to be necessary due to limitations of the semiempirical AM1 method (e.g., it often gives large errors for calculating reaction enthalpies, barriers and basicities[45]). Previously, however, it was only possible to perform gas phase, single point QM calculations to correct the energies for structures optimized at the semiempirical QM/MM level. In another QM/MM study (using MP2/6-31+G(d) energies calculated from HF/3-21G geometries) an alternative mechanism was found, involving initial transfer of a proton from Lys73 to Glu166, through the catalytic water molecule and Ser70. This gives unprotonated Lys73 and protonated Glu166, predicted by those calculations to be the energetically favored state. Tetrahedral intermediate formation was found to occur subsequently in a concerted general base process, with Lys73 promoting Ser70 addition to the β-lactam carbonyl.[26]

Here, we apply a high level QM/MM approach[46] to optimize structures for the reaction, with energies calculated at several levels of theory (e.g., high-level correlated ab initio molecular orbital methods capable of high accuracy), including SCS-MP2/aug-cc-pVDZ//B3LYP/6-31+G(d)/CHARMM27. We test the effects of varying basis set and compare different levels of QM/MM calculation. Calculation of the entire potential energy surface for the formation of the tetrahedral intermediate provides QM/MM energetics and structures at the highest level that should be significantly improved over previous lower level studies (e.g., which used AM1 or HF/3-21G level QM/MM methods, both of which have significant limitations, especially in the calculation of activation barriers).[26,37,38]

The function of Lys73 in class A β-lactamases has been a topic of wide debate. As mentioned above, Lys73 has been shown experimentally to be one of the most important residues for acylation besides Glu166 and Ser70. We investigate this question here by calculating the effects of the Lys73 side chain on the formation of the tetrahedral intermediate in our model, as a first approximation to studying the reaction in a K73A TEM-1 mutant.[15,16,24,29−31,47] We also investigate the effects of the presence of substrate by modeling the activation step in the absence of a substrate in the active site.

Computational Details

High level QM/MM calculations for structure optimization were performed using the program *QoMMMa*,[48,49] which has been developed in-house and couples a quantum chemical package (in this case the program *Jaguar* (Schrödinger, Portland, OR[50]) with the *Tinker* MM software (Software Tools for Molecular Design, St. Louis, MO[51,52]). The CHARMM27 all-atom force field was used to describe molecular mechanical atoms in the calculations.[53] All geometry optimizations were performed at the B3LYP/6-31+G(d)/CHARMM27 level: this hybrid density functional theory treatment should provide reliable structures for the reaction. Hybrid density functional theory methods such as B3LYP provide a good description for many reactions: barriers and reaction energies are typically significantly closer to experiment than those calculated with semiempirical methods, such as AM1.[54] Similarly, B3LYP barriers for reaction are generally much closer to experiment than Hartree−Fock results. However, many DFT-based methods underestimate some reactions barriers by several kcal mol^{-1}.[46,55] Higher level correlated ab initio methods such as MP2 and CCSD give a better treatment of electron correlation and hence generally more accurate energy barriers. The quantum chemistry program *Molpro* (Molpro 2006, Cardiff, U.K.[56]) was used to perform higher level single point energy calculations on the optimized structures, with the largest basis set used consisting of aug-cc-pVTZ for heteroatoms, cc-pVDZ for hydrogens, and cc-pVTZ for carbon atoms. This basis set will be referred to in the remainder of this work as modVTZ. A smaller basis set, referred to subsequently as modVDZ, consists of aug-cc-pVDZ for heteroatoms and cc-pVDZ for hydrogen and carbon atoms. In the spin-component-scaled (SCS) MP2 method,[57] the correlation energy contributions from parallel- ($\alpha\alpha$, $\beta\beta$, "triplet") and antiparallel-spin ($\alpha\beta$, "singlet") pairs of electrons are scaled separately. SCS-MP2 reduces the overestimation of the correlation energy. It is a significant improvement over MP2 in the accuracy of calculated reaction enthalpies.[57]

The substrate complex used as the starting geometry was an AM1/CHARMM27 QM/MM optimized substrate complex (Michaelis complex, MC) from previous calculations.[38] The model is based on a high (1.7 Å) resolution X-ray structure of the E166N mutant of the *E. coli* class A β-lactamase TEM-1 bound to benzylpenicillin (PDB[58] entry code 1FQG[15]). As described fully previously, this structure was remutated in silico to generate the wild type. The model was solvated and truncated by deleting every residue without at least one atom within a 18 Å radius sphere around the hydroxylic oxygen of Ser70 (see ref 38 for a detailed description). In a QM/MM calculation, a QM region must be defined, containing the atoms to be treated quantum mechanically.[12,59] This region must include all atoms that are directly involved in the reaction. It may sometimes also be desirable to include groups believed to have an important (e.g., electrostatic) influence on the reaction, although the number of atoms included in the QM region (QM atoms) is often the primary factor determining computing time, and so may place practical restrictions on the size of the QM region. The QM region used here is somewhat smaller than our previous lower-level QM/MM modeling, which also included the Lys73 and Ser130 side chains.

In our QM/MM treatment of the TEM-1 β-lactamase, the QM region consists of the entire benzylpenicillin substrate, hence a fully active antibiotic, the catalytic (crystallographically observed) water molecule (number 290 in the PDB file for TEM-1, code 1FQG) and side chain atoms of Ser70 and Glu166 (the total net charge of the QM region was $-2e$). It was not possible to include Lys73 in the QM region because of the computational demands of the high-level calculations: these limited the number of atoms that could be treated by QM. Two hydrogen 'link atoms' were added

to saturate the valences of atoms covalently bonded to MM atoms, such that Ser70 was modeled as methanol and Glu166 as acetate,[42,60] and corresponding MM charges were adjusted to preserve total charge. The whole system consisted of 56 atoms in the QM region and a MM region of 3228 protein and water molecule atoms. Every atom further than 18 Å from the reaction center (the hydroxylic oxygen of Ser70 in the starting structure) was held fixed throughout every calculation. Starting from a lower level (AM1/CHARMM27) optimized geometry that was used in previous studies, the energy of the Michaelis (enzyme−substrate) complex was initially minimized without any other restraints or constraints. This newly optimized structure of the Michaelis complex was used as the starting geometry for the calculation of the potential energy surface for the formation of the tetrahedral intermediate (TI). In the presentation of results, the energy of the (optimized) Michaelis complex is taken as the reference energy; thus all calculated energies are given relative to the energy of the optimized substrate complex.

We have shown in previous calculations, testing several different reaction coordinates and combinations of them, that for the acylation, involving Glu166 as general base, a combination of reaction coordinates is required to capture the concerted character of the acylation step.[37,38] We combine two restrained reaction coordinates for the calculation of the potential energy surface, of the type previously used successfully in modeling enzyme mechanisms.[17,27,38,61−63] The first is a complex reaction coordinate (R_{YZ}), which models two processes: the proton transfer from Ser70 to the water molecule 290 and the nucleophilic attack on the β-lactam carbonyl group. This reaction coordinate (R_{YZ}) was defined as the difference between (1) the sum of the interatomic distances between the hydroxyl proton of Ser70 and the accepting oxygen of the water molecule and the Ser70 oxygen to the carbonyl carbon, and (2) the distance between the proton and the Ser70 oxygen ($R_{YZ} = d[O^2{:}H^1] + d[O^1{:}C^1] - d[O^1{:}H^1]$; see Scheme 1). This combined definition of two processes in one reaction coordinate leaves the system the freedom to satisfy this restraint at every step of the simulation, with both events occurring either in a concerted or in a more sequential manner. We have found this reaction coordinate to be effective in previous modeling work.[37,38] The other reaction coordinate (R_X) describes the proton transfer from the water molecule 290 to Glu166 and is defined as the difference between (the interatomic distance of the accepting oxygen of Glu166 to the proton) and (that between the donating oxygen of the water molecule to the moving proton): ($R_X = d[O^3{:}H^2] - d[O^2{:}H^2]$; see Scheme 1). A force constant of 1000 kcal Å^{-2} mol^{-1} was applied to restrain the atoms harmonically to the reaction coordinate values, which were decreased in steps of 0.1 Å. The geometries were optimized at every point of the potential energy surface with respect to the values of the two reaction coordinate restraints. Reaction energetics are obtained by removing any energy contribution from the reaction coordinate restraints (the resulting energies are referred to as single point energies). Through the application of a harmonic restraint with a moderate force constant for the reaction coordinates, the optimized geometries do not always comply exactly with the applied reaction coordinate values (very small deviations up to 0.007 Å were encountered). This was accounted for by considering only the exact reaction coordinate values of the geometries in the generation of the potential energy surface by interpolation. The geometry of the tetrahedral intermediate was additionally optimized without any restraints. For the calculation of the reaction in the wild-type enzyme, we performed in total 205 B3LYP/6-31+G(d)/CHARMM27 geometry optimizations, each of which required about 35−50 h CPU time on a Linux cluster computer system. The large number of optimized structures allows reliable interpolation to construct the overall potential energy surface, and thus the identification of the lowest energy pathway and associated structures that allow conclusions about the underlying reaction mechanism.

Given that the B3LYP QM/MM method gave results comparable to the more expensive ab initio QM/MM methods (see Results below), we used this approach to model two more reactions and calculated the corresponding potential energy surfaces to shed light on substrate effects and the electronic effect of Lys73. First, we modeled the activation of Ser70 in the absence of a substrate in the active site to investigate the influence of the substrate on Ser70 activation. For the calculation of the corresponding surface, the atoms of benzylpenicillin were removed from the Michaelis complex, resulting in a QM region of only 16 atoms (with total charge $-1e$). After an initial geometry optimization, the potential energy surface for the two proton transfers for activation of Ser70 (X and Y; see Scheme 1) was calculated using two reaction coordinates (also at the B3LYP/6-31+G(d)/CHARMM27 level of theory). R_X was kept unchanged for these calculations, whereas the other reaction coordinate R_Y did not include the nucleophilic attack of Ser70 (because the substrate was not present) in this case ($R_Y = d[O^2{:}H^1] - d[O^1{:}H^1]$; see Scheme 1).

Second, the reaction in a mutant (K73A) was modeled to investigate the effect of Lys73 on the formation of the tetrahedral intermediate. A K73A mutant was generated from the optimized Michaelis complex structure of the wild type. This was done by transforming the γ-carbon of Lys73 into a hydrogen and deleting all other atoms of Lys73 that do not occur in an alanine residue. The starting geometry for the mutant enzyme calculations was obtained by an initial optimization of the position of the created hydrogen (all other atoms fixed) followed by a B3LYP/CHARMM27 QM/MM geometry optimization of the system (with boundary atoms fixed as in our previous calculations). The potential energy surface for the K73A acylation was calculated using the same setup and reaction coordinates as for the wild-type enzyme potential energy surface calculations as described above. This "deletion" approach is similar to previous decomposition analyses of contributions of MM residues to calculated QM/MM energy profiles for enzymes,[64−67] including in previous calculations on acylation of the TEM-1 enzyme.[38] See in particular discussion of the analysis of transition state stabilization in *para*-hydroxybenzoate hydroxylase in ref 68. The aim of this approach is to obtain, to a first approximation, an indication of the influence of a particular residue on the calculated reaction energetics. This approach will not create a structural model of the (K73A) mutant protein: that would require solvation and equilibration of the mutated structure, nor do we seek to calculate the effects of the mutation on the overall rate of reaction. Rather, we seek to explore whether the Lys73 side chain has a significant stabilizing effect on the key step of tetrahedral intermediate formation.

The energetics for formation of the tetrahedral intermediate in the wild type enzyme were corrected by calculations at higher levels of theory as follows: the QM and MM coordinates were extracted from the B3LYP/6-31+G(d)/CHARMM27 optimized structures. The coordinates were used to recalculate QM/MM single point energies with several higher level quantum mechanical methods for the QM atoms, including the CHARMM27 charges of the MM atoms in the QM Hamiltonian. In total we calculated three entire corrected QM/MM surfaces using SCS-MP2/modVDZ, MP2/modVDZ, and HF/modVDZ as the QM

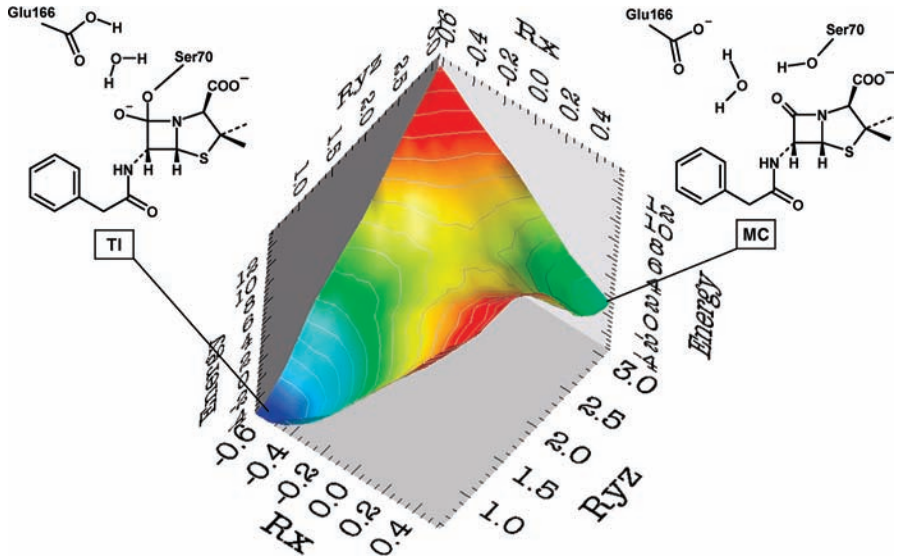

Figure 1. B3LYP/6-31G+(d)/CHARMM27 QM/MM potential energy surface for formation of the tetrahedral intermediate in acylation. MC is the Michaelis (enzyme−substrate) complex; TI is the tetrahedral intermediate. The energy is given in kcal mol^{-1} and the reaction coordinates R_X and R_{YZ} in Å.

methods. Furthermore, we recalculated the energies for the three most important structures of the reaction, that is, the Michaelis complex (MC), the transition state (TS), and the tetrahedral intermediate (TI) using bigger basis sets, up to the SCS-MP2/modVTZ level. It is worth emphasizing that the pVDZ and pVTZ basis sets are significantly more computationally intensive than the simple 6-31G+(d).

Results

The B3LYP/6-31+G(d)/CHARMM27 potential energy surface for the formation of the tetrahedral intermediate in the wild type TEM-1 enzyme is shown in Figure 1. The lowest energy path from the Michaelis complex (MC: R_X[0.57 Å]; R_{YZ}[3.05 Å]) to the tetrahedral intermediate (TI: R_X[−0.53 Å]; R_{YZ}[0.7 Å]) goes approximately diagonally through the middle of the surface. No stable intermediate structure (i.e., energy minimum) is predicted between the reactants and tetrahedral intermediate. The route of the lowest energy path through the middle of the surface indicates that the reaction proceeds via a concerted mechanism. Stepwise paths have considerably higher energy: a pathway along either single reaction coordinate R_X or R_{YZ} leads to areas of highest energy, which correspond to unstable high energy structures (e.g., R_X[0.57 Å];R_{YZ}[1−0.7 Å] and R_X[−0.4−0.6 Å];R_{YZ}[3.05 Å]).

Overall the potential energy surface has a very smooth shape, indicating that the applied reaction coordinates and modeling procedure capture the essential details of the reaction correctly. No other chemical changes were observed and structural changes of the enzyme during the reaction are relatively small. The energy profile along reaction coordinate R_{YZ} shows complex behavior, with, e.g., a larger slope between 0.8 and 1.5 Å, indicating that the two reactive processes involved in this coordinate (Y and Z; see Scheme 1) do not occur synchronously. The barrier for formation of the tetrahedral intermediate can be estimated as 4.5 kcal mol^{-1} from the energy of the transition state (TS), i.e., the highest energy point along the lowest energy path (R_X[−0.03 Å]; R_{YZ}[2.35 Å]). The tetrahedral intermediate has a significantly lower energy than the Michaelis complex of −5.4 kcal mol^{-1}, i.e., predicting that formation of the TI is exothermic.

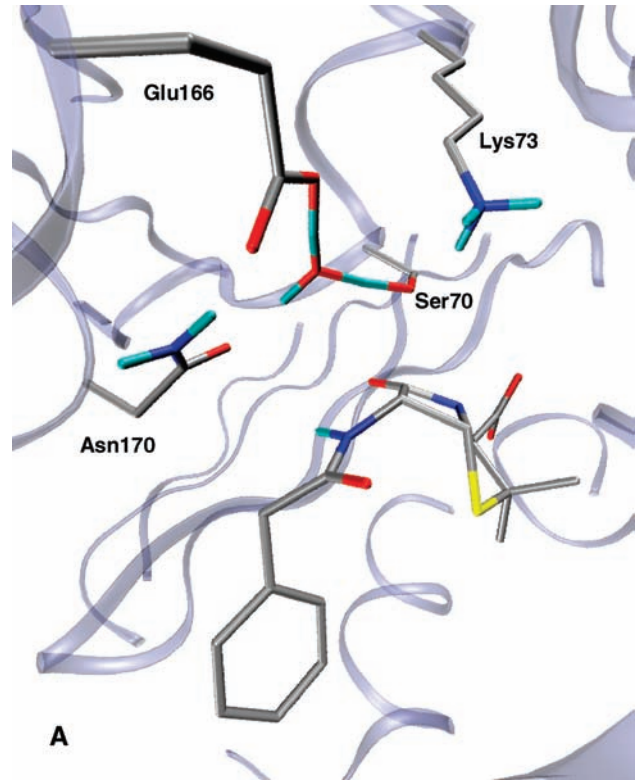

Figure 2. B3LYP/6-31G+(d)/CHARMM27 transition state structure, showing some important residues. Glu166 deprotonates an ordered water molecule, which deprotonates Ser70. The distance between the β-lactam carbon and the hydroxyl of Ser70 is reduced to 2.37 Å in the TS. Carbon atoms are gray, oxygens are red, sulfur are yellow, hydrogens are cyan, and nitrogens are blue.

The B3LYP/6-31+G(d)/CHARMM27 transition state structure is shown in Figure 2. The two protons transferred during Ser70 activation are almost equidistant between the respective accepting and donating oxygens: the distance between the accepting carboxylate oxygen of Glu166 and the transferring proton from the water is the same as the distance between that proton and the donating water oxygen (d[O^3:H^2] is 1.2 Å and d[O^2:H^2] is 1.22 Å; see Scheme 1 and Figure 2). Also the proton−oxygen distances of the transfer from Ser70 to the water

TABLE 1: Reaction Energetics for Formation of the Tetrahedral Intermediate Calculated at Different Levels of QM/MM Theory[a]

species	basis set	SCS-MP2	MP2	HF	B3LYP
energy of the transition state (kcal mol^{-1}) relative to Michaelis complex (i.e., barrier height)	6-31G+(d)				4.5
	aug-cc-pVDZ	4.5	2.9	12.2	3.4
	aug-cc-pVDZ H = cc-pVDZ, C = cc-pVDZ	5.2	3.6	12.5	
	aug-cc-pVTZ H = cc-pVDZ, C = cc-pVTZ	4.1	2.4	11.8	
energy of the tetrahedral intermediate (kcal mol^{-1}) relative to Michaelis complex	6-31G+(d)				−5.4
	aug-cc-pVDZ	−10.9	−12.5	−2.9	−5.4
	aug-cc-pVDZ H = cc-pVDZ, C = cc-pVDZ	−9.4	−10.9	−2.7	
	aug-cc-pVTZ H = cc-pVDZ, C = cc-pVTZ	−9.5	−11.2	−1.7	

[a] Energies for the transition state and the tetrahedral intermediate are given relative to the energy of the Michaelis (substrate) complex. The structures correspond to the key points on potential energy surfaces calculated at each different QM level by single point QM/MM calculations on structures from a B3LYP/6-31G+(d)/CHARMM27 potential energy surface calculation (see text for details). Where no number is shown, the calculation was not performed.

molecule are similar (d[O^2:H^1] is 1.2 Å and d[O^1:H^1] is 1.23 Å; see Scheme 1 and Figure 2). The distance between the carbonyl carbon and the attacking oxygen (d[O^1:C^1]; see Scheme 1) decreases by 0.18 Å from 2.55 Å in the Michaelis complex to 2.37 Å at the transition state, much longer than the equilibrium length of the bond to be formed (1.55 Å in the tetrahedral intermediate). The geometry of this carbonyl carbon has changed from an ideal planar sp^2 conformation in the Michaelis complex with the carbonyl oxygen a little out of plane. No stable intermediate with Ser70 deprotonated is observed at any position on the potential energy surface when a substrate is present in the active site.

The potential energy surfaces calculated with other levels of QM/MM theory (HF/modVDZ/CHARMM27, MP2/modVDZ/CHARMM27 and the SCS-MP2/modVDZ/CHARMM27) are all qualitatively similar to the B3LYP QM/MM surface (data not shown). The MP2, SCS-MP2, and B3LYP QM/MM calculations all gave similar reaction barriers, though the calculated relative energy of the tetrahedral intermediate differs somewhat comparing the B3LYP and MP2 or SCS-MP2 results (see below). The results overall indicate that the B3LYP method treats this reaction reasonably well. The B3LYP results are also relatively insensitive to the basis set used. At the B3LYP/aug-cc-pVDZ level, the TS has an energy relative to the substrate complex (MC) of 3.4 kcal mol^{-1} and the TI a relative energy of −5.4 kcal mol^{-1}. At the B3LYP/6-31+G(d) level, the relative energy of the TS is 4.5 kcal mol^{-1} and that of the TI is −5.4 kcal mol^{-1}. Only the Hartree−Fock method gave significantly different energetics for the modeled reaction, not unexpectedly. The relative energies for the three important species in the reaction (MC, TS, TI) are summarized in Table 1 (because the CHARMM27 force field[53] was always used for the MM part, we refer only to the level of the QM method in the following).

The calculated barriers with all methods except HF are significantly lower than the experimentally derived barrier (12 kcal mol^{-1}). The MP2 barrier is lowest, but all the methods that include electron correlation give barriers of the same magnitude. For instance, the highest level of theory employed, referred to here as SCS-MP2/modVTZ, gives a barrier (4.1 kcal mol^{-1}) very close to the B3LYP/6-31+G(d) result (4.5 kcal mol^{-1}). These methods do, however, differ in their prediction of the relative stability of the TI. All the methods predict the TI to be more stable than the substrate (all calculate the QM/MM energy of the TI to be lower than that of the substrate). The B3LYP/6-31+G(d) method appears to underestimate the stability of the TI (−5.4 kcal mol^{-1}) relative to the substrate, compared to the high-level ab initio QM/MM calculations with SCS-MP2 or MP2 methods (relative energies of TI from −9.4 to −12.5 kcal mol^{-1}, Table 1).

The influence of the substrate during Ser70 activation was investigated by modeling the two proton transfers for activation of Ser70 in the absence of the substrate (X and Y Scheme 1) at the B3LYP/6-31+G(d)/CHARMM27 QM/MM level (only). We found that the calculated barrier did not change compared to the activation of Ser70 in the presence of benzylpenicillin. In this hypothetical model, the resulting, activated structure after the two proton transfers contains deprotonated Ser70 and is marginally less stable than the Michaelis complex (by 0.3 kcal mol^{-1}). It should be noted that this structure is somewhat artificial, as the void left by deletion of the substrate is not filled by water molecules, and the protein structure is essentially unaltered from the substrate complex. Thus we do not regard this as an estimate of the true energy cost for deprotonating Ser70 in the apo enzyme; these calculations are intended to test the effect of the presence of the substrate in the structure used here.

The acylation in the K73A mutant with benzylpenicillin was modeled exactly as for the wild type (a potential energy surface was calculated at the B3LYP/6-31+G(d)/CHARMM27 level with the same two reaction coordinates). The general shape of the potential energy surface for formation of the TI with the K73A mutant was similar to the wild type potential energy surface (data not shown, compare Figure 1); i.e., the lowest energy path still goes through the middle of the potential energy surface with no additional minima observed other than the TI. However, the reaction energetics change slightly: the barrier is 6.2 kcal mol^{-1}, 1.7 kcal mol^{-1} higher than the wild type.

The transition state structure in the K73A mutant is generally similar to that calculated for the wild type, although there are a few differences: the distance between the moving proton and the oxygen of Ser70 (1.18 Å) is slightly shorter than the distance between these two atoms in the TS of the wild type (1.23 Å). Also the distance between the accepting oxygen of Glu166 and the transferring proton of the water molecule (1.1 Å) is shorter in the mutant TS than in the TS of the wild type where the distance is 1.2 Å (see Figure 2).

Discussion

The chemical mechanism postulated for the formation of the tetrahedral intermediate in the acylation step of TEM-1 by

benzylpenicillin revolves around Glu166 as the general base.[37,38] In this mechanism, Glu166 activates Ser70 through a hydrogen bond network: Glu166 deprotonates a conserved water molecule, which in turn deprotonates Ser70 (see Scheme 1). The potential energy surface calculated for TEM-1 β-lactamase acylation at the B3LYP/6-31+G(d)/CHARMM27 level has a very smooth shape indicating that the applied reaction coordinates model the process of TI formation well. This is indicated by the fact that no processes which are not defined in the two applied reaction coordinates are encountered, which would cause "edges" or discontinuities in the surface due to large energy drops. The lowest energy path leads directly from the Michaelis complex to the TI, which is lower in energy; i.e., the first step of the acylation reaction happens in a concerted manner and is exothermic. This finding supports the conclusion of two lower level QM/MM studies.[26,37,38]

Higher level calculations, up to the SCS-MP2/modVTZ/CHARMM27 level (the highest level of quantum chemical theory applied to the β-lactamase reaction to date), support the conclusions drawn from the B3LYP/6-31+G(d)/CHARMM27 results. With the exception of the Hartree−Fock results, all the calculated barriers are in the same range (the highest level calculations predict a barrier of 4.1 kcal mol^{-1}). Furthermore, the position of the TS on the potential energy surfaces obtained with HF, MP2, or SCS-MP2 QM/MM methods is very similar to what is observed on the B3LYP/CHARMM27 surface. The nucleophilic attack in the TS here is slightly more advanced than in our previous lower level study of TEM-1.[38] The calculated barriers with all the correlated QM/MM methods are significantly lower than the experimental value of about 12 kcal mol^{-1} (derived from the rate of cleavage of benzylpenicillin by TEM-1, estimated from k_{cat} by transition state theory).[24,69−72] On the face of it, this might indicate that this step is in fact not rate limiting, or that there are limitations in the modeled mechanism or in the model studied. However, the results here are not definitive enough to draw such conclusions with confidence. One should be cautious about making direct comparisons between experimental free energy barriers and potential energy barriers.[63] Experimental free energy barriers contain the effects of entropy, and zero-point (and thermal) vibrational energy differences. The former are expected to increase the barrier relative to the potential energy barrier (i.e., the free energy barrier is likely to be somewhat higher than the potential energy barrier), whereas the latter would decrease the barrier. For example, QM/MM calculation of the potential energy barrier for the hydroxylation reaction in *para*-hydroxybenzoate hydroxylase revealed that it was smaller (22.8 kcal mol^{-1}) than the free energy barrier (25.9 kcal mol^{-1}) obtained with the free energy perturbation method.[73] However, typically for enzyme reactions, the difference between the energy barrier and the free energy of activation for the catalytic step is fairly small.[46] Quantum tunneling is potentially important in reactions involving proton transfer, and could also reduce the effective barrier somewhat.[67,74−77] It is also important to remember that experimental (e.g., steady state) rates may refer to overall rates of reaction rather than that for a single chemical step. The apparent activation free energy is an effective upper limit with which to compare a calculated activation energy for any single step. The barriers here appear somewhat too low but are not inconsistent with experimental results. Another very important factor is that only a single conformation of the protein is considered here—the effects of conformational averaging are not included. Relatively small changes in structure can cause significant changes in calculated barriers.[46,49,61,78] Different conformations would be likely to show significantly different degrees of stabilization of the TI, for example. The TI here is found to be very stable, more stable than the substrate complex. The height of the barrier is likely to be related to the relative stability of the TI, so other conformations might well show higher barriers. Conformations with lower barriers would be expected to dominate the reaction, but only if the energetic cost of forming such conformations is relatively low compared to the difference in barriers between conformations.[61] More extensive study would be required to determine the free energy cost of tetrahedral intermediate formation in the TEM-1 enzyme.

As expected, the energetics obtained from Hartree−Fock QM/MM calculations differ significantly from B3LYP, SCS-MP2, and MP2 results (Table 1). The calculated Hartree−Fock QM/MM barriers are about ∼12 kcal mol^{-1} and coincidentally match the experimental activation energy of 12 kcal mol^{-1}. The fact that the Hartree−Fock QM/MM energy barrier apparently agrees well with experiment certainly does not show that this method is the best of those applied here. The B3LYP, MP2, and SCS-MP2 methods are an improvement on the HF method due to their inclusion of electron correlation. However, MP2 and B3LYP methods sometimes underestimate reaction barriers somewhat, e.g., for some proton transfers.[46,79−82] There is also some variation between the methods in the predicted stability of the TI, though all predict that it is more stable than the substrate complex, as discussed below. The tetrahedral intermediate also is predicted to be less stable at the Hartree−Fock level (−1.7 kcal mol^{-1} at the HF/modVTZ level) compared to methods that include electron correlation (−9.5 kcal mol^{-1} at the SCS-MP2/modVTZ level).

The structure of the TS (Figure 2), which is mostly similar to that previously reported at the AM1 level,[38] shows the two transferring protons almost equidistant between their respective donating and accepting atoms. The proton transfer "relay station",[38] the water molecule (number 290), is stabilized and held in its position throughout the reaction by a hydrogen bond to the carbonyl oxygen of the side chain of Asn170, an important residue that has been found experimentally to be indispensable for the hydrolysis of imipenem β-lactam antibiotics.[38,83] The study by Smith et al. reports[83] that a Gly170Asn point mutation on the GES-1 β-lactamase resulted in an enzyme (labeled GES-2) that exhibited little change in catalytic rate (k_{cat} increased from 0.003 to 0.004 s^{-1}) but a 100-fold decrease in K_m with imipenem, from 45 to 0.45 μM. This was thought to be partially due to Asn170 forming a hydrogen bond with the conserved water molecule. The water molecule also interacts with the other residues involved in the proton transfers (Glu166 and Ser70). On the basis of interatomic distances, the Ser70-penicillin bond is only just starting to be formed at the TS. It is apparent that deprotonation of Ser70 is energy demanding, while subsequent nucleophilic attack is relatively facile. This has been observed in other enzymes such as fatty acid amide hydrolase, where the TS corresponds to the deprotonation of the serine rather than the nucleophilic attack.[27] After the TS, the proton from Ser70 moves more than 1.45 Å away from the Ser70 oxygen and the nucleophilic attack forming the tetrahedral intermediate happens quickly.

In the TS, the slightly deprotonated Ser70 interacts in the beginning of the nucleophilic attack with the positively charged Lys73 that donates a hydrogen bond to Ser70 (2.7 Å distance between the Lys73 ζ-nitrogen and Ser70 hydroxylic oxygen in the TS; see Figure 2). As found in our earlier, lower level QM/MM calculations, the oxyanion hole provides increasing stabilization of the reacting system as the reaction proceeds (as

negative charge increases on the carbonyl oxygen):[38] it stabilizes the TS relative to the substrate but stabilizes the TI most of all, because the negative charge of the oxygen is greatest at the TI. Lys73, on the other hand, appears specifically to stabilize the TS. Interestingly, a similar finding was reported in fatty acid amide hydrolase,[61] where Lys241, similarly to Lys73 in TEM-1, stabilizes the TS for proton transfer between the two serine residues, equivalent to the proton transfer between Glu166 and the water molecule in TEM-1. In fatty acid amide hydrolase, the positioning of the lysine side chain is found to be important in determining the barrier to reaction, with different active site conformations showing significantly different barriers to reaction.[61] Similar effects could be important in TEM-1. The high computational expense of the QM/MM methods applied here precluded the examination of reaction in multiple conformations of TEM-1.

The modeling of the activation of Ser70 in the absence of the substrate gave a barrier (4.8 kcal mol^{-1}) that is (perhaps surprisingly) very similar to that when the substrate is in the active site (4.5 kcal mol^{-1}, Table 1). This indicates that the benzylpenicillin substrate has very little influence on the deprotonation reaction energy. The proportion of deprotonated Ser70 in the free enzyme is likely to be vanishingly small, as expected.

All the methods predict the tetrahedral intermediate to be more stable than the substrate in the enzyme, corresponding to an exothermic reaction. This indicates a descending energy profile (if indeed acylation is the most significant barrier and the other steps follow the pattern found in our previous calculations[17]), which has been proposed to be expected for well-evolved enzymes that catalyze exergonic reactions.[84,85] We have previously calculated the energy profile for the entire reaction at a lower level of theory[17] and would expect the energy profile for the whole reaction (i.e., including steps beyond tetrahedral intermediate formation) to be similarly downhill if calculated at a higher level for our model. There is of course uncertainty in the calculated relative energy of the tetrahedral intermediate: this energy, like the barrier, will be sensitive to details of the model (see below). In contrast, Meroueh et al. found endothermic reaction energetics for the formation of the TI, though this in itself does not constitute evidence for either mechanism.[26] QM/MM studies of the formation of a tetrahedral intermediate as the first step of an acylation reaction found similar endothermic reaction energetics in the case of NS3 protease[86] and fatty acid amide hydrolase.[27] The relative stability of the TI is likely to be determined by the conformation of the enzyme and the (perhaps subtle details of the) positioning of the substrate in the oxyanion hole. Further sampling of conformations would be required to establish the relative stability of the TI in TEM-1.

The barrier for the nucleophilic attack found here is low, and this is almost certainly related to the calculated stability of the TI (both facts could be significantly different for other configurations of the enzyme in calculations at the same level). It is worth pointing out that barriers for similar (e.g., for amides) nucleophilic attack reactions in the gas phase tend to be very low,[87] while barriers to reaction in aqueous solution[88−90] are significantly higher. This does not mean, however, that the reaction in the enzyme should be equated with a gas phase reaction; the "desolvation" hypothesis has been discussed in detail elsewhere.[59,91] In the enzyme, polar groups are oriented to supply significant stabilization of the reacting species, and are specifically organized and positioned to provide catalysis (i.e., better stabilization and thus a lower barrier than for an equivalent reaction in solution).[59,91] The small barrier found here is in contrast to computational findings for some related enzyme-catalyzed reactions such as zinc-dependent β-lactamases[92] (but see also ref 93) and peptidases;[94,95] the predicted high relative stability of the tetrahedral intermediate also contrasts with some findings for other enzymes as mentioned above. Detailed comparison with other enzymes and of the effects of protein and solvent structural configurations and different computational techniques will be useful in analyzing the causes of these differences.

The most important finding here though does not depend crucially on the exact value of the calculated barrier, nor on the apparent stability of the tetrahedral intermediate: that is, the results show that the proposed mechanism of acylation with Glu166 as the base is certainly energetically feasible, and the active site of the TEM-1 is structurally well organized to catalyze the reaction via this mechanism.

In the study by Meroueh et al. an alternative reaction path was proposed,[26] on the basis of a stable intermediate structure in which an acidic residue (Glu166 in its protonated form) and a basic residue (Lys73 in its neutral form) are in close proximity. These workers calculated MP2/6-31+G(d) single point energies at HF/3-21G optimized geometries. In our current and previous[17,37,38] modeling, we have found no evidence for such a species, and it seems energetically improbable. It seems unlikely that similar substrates (such as penicillanic acid used in that study and benzylpenicillin used here) are turned over with different reaction mechanisms, although it is possible that the mechanism may not be unique: alternative possible mechanisms (e.g., for different substrates) could perhaps give the lactamase a degree of catalytic robustness, e.g., allowing it to be promiscuous and accept a wide variety of substrates. The acylation barrier of about 22 kcal mol^{-1} calculated in the study of Meroueh et al. is notably higher than the apparent experimental value of around 16−17 kcal mol^{-1} (Note that this is for hydrolysis of penicillanic acid by TEM-1, which is slower than that for benzylpenicillin). On the face of it, this argues against that proposed mechanism, but this difference in activation energy is not conclusive given the factors discussed above that can affect comparison of calculated and experimental activation energies. The methods applied by Meroueh et al. are likely to give reasonably good energetics for the reaction (MP2/6-31+G(d) energies calculated for HF/3-21G optimized geometries). Though the energy calculation methods (MP2) are comparable to those applied here, there are differences between the QM/MM approaches applied here and in their study, which could be important. The TI and TS found by Meroueh et al. are significantly less stable (relative to the reactant complex) than we find here: our TS is 18−20 kcal mol^{-1} relatively lower than theirs, and our TI is 23−25 kcal mol^{-1} lower than theirs. It is difficult to identify precisely the origin of the differences observed here in the calculated energetics. It seems unlikely that either the different substrates or the higher basis sets used by us (up to modVTZ) compared to the basis set used by Meroueh et al. (6-31+G(d)) are responsible for these large differences. It is possible that the use of a different QM level of geometry optimization (HF/3-21G), or the differences in the applied reaction coordinates, are related to these apparent stability differences. Other possible factors that could give rise to differences include the QM/MM treatment, including long-range electrostatic interactions. Most important is likely to be the use of different structures (including different positioning of solvent molecules) and (perhaps) different protonation states:

for a complex system such as a protein, even slightly different structures may give significantly different energetics (e.g., different barriers) for a mechanism,[49,63,78,96] and thus complicate the comparison of different mechanisms. Similarly, different initial models (e.g., differing in protonation states for ionizable residues, or solvation) may well produce significantly different results. Ionizable residues in proteins may have pK_a values significantly altered from those expected in solution, and they may play unexpected roles in biochemical mechanisms (e.g., arginine acting as an acid[62]); thus mechanisms involving "nonstandard" protonation states should not be ruled out in advance. To rule out a mechanism with confidence, it would be important to include conformational effects (e.g., sampling protein conformations by molecular dynamics[63]) and other important contributions and show that the barrier was higher than the experimental finding by an amount that is significant for the computational method.[97] This cannot yet be shown for the TEM-1 β-lactamase, and further study is required for definitive conclusions. Our results do show that our proposed mechanism (involving Glu166 as the base for acylation) is structurally and energetically reasonable and is consistent with experimental kinetic and structural data.

Of course, the choice of QM and MM regions (and indeed the choice of initial protonation states for residues in both regions) restricts the type of mechanism that can be modeled and dictates the calculated energetics. Treating Lys73 by MM precludes its direct involvement in proton transfer here. This choice was made because the computational demands of the high level QM/MM calculations limited the number of atoms that could be treated by QM. Without specific modeling or definitive experimental data, one cannot definitively rule out a mechanism. It is possible, though, to perform calculations to show that a mechanism is reasonable.[97] A mechanism that is found to have an extremely high energy barrier in a realistic model can be concluded safely to be unlikely, while a mechanism with a reasonable barrier (not significantly higher than the apparent barrier derived from experimental rates) may be regarded as reasonable and consistent with experimental data. The barrier found here is notably lower than the apparent barrier from the overall rate: this could indicate that the acylation is not in fact rate limiting or could be due to the structure used (the exact barrier will vary significantly depending on the protein/solvent configuration used for potential energy barrier calculations), or to some details of the model or mechanism being incorrect, or to weaknesses in the theoretical methods. At the relatively high level of QM/MM theory applied here, one can discount significant errors in the energy barrier for a reaction of this type due to the QM method.[46] We believe that the structural model used for the enzyme here is reasonable, in line with experimental data. It should also be noted again that the calculated barrier here is a potential energy barrier and does not include the activation entropy (nor tunnelling, zero-point or thermal vibrational effects).

TEM-1 β-lactamase is important not only because of the medical relevance of this enzyme class but now also as a model system for testing computational molecular modeling methods. Other important model enzymes include chorismate mutase,[46,49,64,78,96] citrate synthase,[62,65] *para*-hydroxybenzoate hydroxylase,[46,68,73] and cytochrome P450cam:[63,98] such "guinea pig" enzymes allow for comparison of different methods and testing how the model setup influences calculated energetics for reactions.[63,98] This can analyze uncertainties in calculations, and provide error estimates, helping to solidify mechanistic conclusions.[97] High-level QM/MM methods[46,54] of the type applied here provide a benchmark for testing and validating lower-level computational approaches.

All of our calculated energetics obtained from several high-level QM/MM methods give consistent results that are quantitatively very similar and qualitatively identical, leading to the same conclusions consistent with experimental data (It is important to point out that the experimental rate for this single step is unknown, and so a direct comparison with experiment can only be made for the overall reaction; we conclude that this step is energetically feasible and lower than the apparent experimental barrier, which in turn may relate to a single chemical rate-determining step, widely believed to be associated with acylation). All the methods that include electron correlation are well suited to model the formation of the tetrahedral intermediate and to calculate the corresponding potential energy surface, because the energies of unstable species and transition states are particularly sensitive to the treatment of electron correlation. While the calculated energetics (including the relative stability of the TI) are expected to be somewhat sensitive to the structure of the protein used, our calculations show that the proposed mechanism in which Glu166 acts as the base, via a conserved water molecule, to deprotonate the nucleophilic Ser70 can occur (in a detailed model of the enzyme) without structural reorganization and with low barriers.

It has been proposed that Lys73 stabilizes Ser70 during its deprotonation. We investigated this by calculation of a potential energy surface with Lys73 mutated to alanine.[31,38] As noted in the Computational Details, this does not model the structural or solvation changes associated with the mutation: the calculations given an indication of the contribution of Lys73 to the calculated energetics here. We found a slightly increased barrier for this mutant, which lacks the positive charge of Lys73 in the active site. As shown in our previous semiempirical QM/MM study, in the course of Ser70 deprotonation, the negative charge of the deprotonated Ser70 oxygen increases.[38] The positive charge of the ζ-ammonia group of Lys73 is well located to stabilize this negative charge (see Figure 2). This stabilizing effect is missing in the K73A mutant model, giving an increased barrier for acylation in the mutant. Furthermore, the transition state structure reveals that the abstracted proton from Ser70 is more tightly bound to Ser70 in the mutant TS.

Our calculations (including previous QM/MM modeling of the deacylation reaction) indicate that Lys73 plays an important role as a proton shuttle in subsequent reaction steps (in both acylation and deacylation).[24,38,99] The observed decreased acylation rates in K73 mutants are most likely a consequence of both the lack of transition state stabilization during Ser70 activation found here and the inability to transfer protons efficiently within the active site in subsequent reaction steps. These functions of Lys73 in acylation, as well as its proposed role in deacylation may explain its strict conservation in the class A β-lactamase family.[17]

This work shows that QM/MM calculations can be performed for enzyme reactions using high level correlated ab initio QM/MM methods with reasonably large basis sets. The calculated energetics for the reaction are not very sensitive to the basis sets used. Given that class A β-lactamase mechanisms certainly warrant further computational investigation in future, it is appropriate to discuss what computational methods and approaches may be most useful (e.g., choice of basis set and modeling or simulation methods). We believe that the most important extension for future QM/MM investigations of class A (and other) β-lactamases should be more conformational sampling and tests of the sensitivity of the results to the

structural model used (and, e.g., the solvation of the system and protonation states). For modeling the reaction by potential energy surface/profile (e.g., adiabatic mapping/geometry optimization/reaction pathway) calculations, multiple conformations (e.g., from MM or QM/MM MD[12,49,96]) should be considered, to investigate the dependence of the results on the starting structure, and the sensitivity of the calculated energies. Adiabatic mapping calculations have well-known limitations for calculating reaction barriers and energies (e.g., in not allowing significant environmental change associated with reaction), and therefore molecular simulations are required for investigations of many enzyme-catalyzed reactions.[63,100,101] Calculations of free energies of reaction, e.g., by umbrella sampling molecular dynamics, perhaps with specifically parametrized semiempirical QM[100] or empirical valence bond[59] methods, will be useful; clearly it will remain impossible for the foreseeable future to perform extensive molecular simulations (e.g., molecular dynamics[100] or Monte Carlo[102]) with correlated ab initio methods[46] for QM regions of the size typically required for modeling enzyme-catalyzed reactions. A larger QM region than that used here (e.g., including Lys73) would be needed to model all the steps of acylation and deacylation,[17] and could be used to study alternative mechanisms, but will increase the computational demands of the calculations. If the aim is to calculate activation energies with high (e.g., approaching "chemical") accuracy,[103] which correlated ab initio methods can potentially provide, then it would also be necessary to consider zero-point energy,[46] quantum tunneling,[67,74] and entropic[46] contributions. For comparison of relative barriers (e.g., for different substrates), such contributions to the barrier may be approximately equal, making comparison of potential energy barriers reasonable.[66,97] Alternative β-lactam substrates and mutant β-lactamase enzymes should be investigated. High-level QM/MM calculations,[46] e.g., using correlated ab initio methods such as the SCS-MP2 results here, should provide useful benchmarks for testing and developing more approximate QM or more empirical modeling methods. QM/MM calculations with density functional (e.g., B3LYP) methods,[104] with relatively small basis sets (e.g., 6-31+G(d) appear to provide a reasonably accurate description of this reaction, though attention should be paid to the calculated relative stability of the tetrahedral intermediate. The results here show that QM/MM calculations at the B3LYP QM level should provide a reasonable compromise in terms of accuracy and speed, allowing fairly extensive calculation of potential energy surfaces. Calculations of reaction free energies with DFT methods such as B3LYP are becoming possible in QM/MM calculations on enzymes, but the necessary simulations (requiring perhaps hundreds of millions of energy (and for dynamics simulations, also force) evaluations) will remain highly computationally demanding. Hartree−Fock ab initio QM/MM calculations perform poorly for the energetics of the reaction (as expected), at a comparable computational cost and are not recommended. Correlated ab initio QM/MM calculations[46] with large basis sets (e.g., single point calculations for energies of crucial points on surfaces calculated with DFT QM/MM methods) will provide a useful test (and energetic corrections) of lower level results.

Conclusions

High level QM/MM calculations (using various QM methods up to the SCS-MP2/modVTZ/CHARMM27 level) have been performed to model the proposed rate-determining step for the formation of the tetrahedral intermediate in acylation of the class A β-lactamase TEM-1 with benzylpenicillin. The results support a mechanism in which Glu166 acts as the general base to deprotonate Ser70 (via an intervening water molecule) for nucleophilic attack on the β-lactam carbonyl group. The calculated barriers are $\sim$4−5 kcal mol^{-1}, which is somewhat too low in comparison to experimental data, but of reasonable magnitude considering that entropic effects are not included and the energies were calculated from a single conformation only. The results show that the proposed mechanism is reasonable. Comparison with correlated ab initio QM/MM calculations shows that the B3LYP hybrid DFT method provides a reasonably good structural and energetic description of this reaction.

The formation of the tetrahedral intermediate consists of three processes: Ser70 deprotonation and transfer of the proton to the catalytic water molecule, proton transfer from this water molecule to Glu166, and nucleophilic attack of Ser70 on the β-lactam substrate. The potential energy surface of the acylation was calculated by applying two reaction coordinates, one of which describes two bond-making/breaking events, thus modeling all three such processes at once. The calculation of the potential surface in this way is important to achieve reliable results for such a highly concerted reaction.

The potential energy surfaces calculated here support previous lower-level findings that formation of the tetrahedral intermediate follows a concerted reaction mechanism.[38] Analysis of the calculated transition state structure reveals that the energy demanding events of these three processes are the two proton transfers for Ser70 activation. The nucleophilic attack of Ser70 on the β-lactam carbonyl carbon is slightly delayed, not synchronous with these proton transfers, although the whole process is clearly concerted. Modeling of the activation of Ser70 in the absence of the substrate gives an almost unchanged barrier. That suggests that the presence of a β-lactam compound does not affect the barrier for Ser70 activation.

The potential energy surface for the formation of the tetrahedral intermediate in the K73A mutant model shed light on the function of the important conserved Lys73 residue. Analysis of acylation in this mutant revealed that the concertedness of the three processes remained unchanged, but the energetics changed noticeably. The results support our previous finding[37] of Lys73 having the important function of stabilization of the TS (and particularly deprotonated Ser70) in the course of Ser70 activation. The barrier for the formation of the tetrahedral intermediate in a K73A mutant model was found to be slightly increased. This is in qualitative agreement with experimental studies[105] that show a decrease in rate when this residue is replaced (the rate constant decreases from 3100 to 1.2 s^{-1} for benzylpenicillin hydrolysis in the K73A mutant, which corresponds to an increase in activation free energy from 12.7 to 17.3 kcal mol^{-1}). Lys73 is calculated here to stabilize the transition state for TI formation in acylation; it is calculated to lower the barrier by 1.7 kcal mol^{-1} corresponding to a roughly 10-fold rate enhancement. In addition to its vital role as a proton shuttle residue in subsequent reaction steps,[17] this function of Lys73 is likely to be one of the reasons for the experimentally observed decreased acylation rates of K73 mutants. The question of the role of K73 deserves further investigation.

The high level QM/MM results presented here support an acylation mechanism involving the carboxylate of Glu166 acting as the general base, deprotonating a structurally conserved water molecule for nucleophilic attack on the β-lactam ring carbonyl carbon.

Acknowledgment. A.J.M. and J.C.H. thank the Royal Society (U.K.) for a visiting Fellowship for J.C.H., A.J.M., J.N.H., and

J.P. also thank EPSRC for support (A.J.M. is an EPSRC Leadership Fellow), and Dr. F. Manby for useful discussions.

References and Notes

(1) Knowles, J. R. *Acc. Chem. Res.* **1985**, *18*, 97–104.

(2) Page, M. I. In *The chemistry of beta-lactams*; Page, M. I., Ed.; Blackie: Glasgow, 1992; p 79−100.

(3) van Heijenhoort, J. In *New Comprehensive Biochemistry. The Bacterial Cell Wall*; Ghuysen, J.-M., Hakenbeck, R., Eds.; Elsevier: Amsterdam, 1994; Vol. 27.

(4) Waxman, D. J.; Strominger, J. L. *Annu. Rev. Biochem.* **1983**, *52*, 825–869.

(5) Massova, I.; Mobashery, S. *Curr. Pharm. Des.* **1999**, *5*, 929–937.

(6) Cohen, M. L. *Science* **1992**, *257*, 1050–1055.

(7) Neu, H. C. *Science* **1992**, *257*, 1064–1073.

(8) Davies, J. *Science* **1994**, *264*, 375–382.

(9) Livermore, D. M.; Woodford, N. *Trends Microbiol.* **2006**, *14*, 413–420.

(10) Bloomfield, S. F.; Cookson, B.; Falkiner, F.; Griffith, C.; Cleary, V. *Am. J. Infect. Control* **2007**, *35*, 86–88.

(11) Diep, B. A.; Chambers, H. F.; Graber, C. J.; Szumowski, J. D.; Miller, L. G.; Han, L. L.; Chen, J. H.; Lin, F.; Lin, J.; Phan, T. H.; Carleton, H. A.; McDougal, L. K.; Tenover, F. C.; Cohen, D. E.; Mayer, K. H.; Sensabaugh, G. F.; Perdreau-Remington, F. *Ann. Intern. Med.* **2008**, *148*, 249–257.

(12) Mulholland, A. J. *Drug Discov. Today* **2005**, *10*, 1393–1402.

(13) Ambler, R. P.; Coulson, A. F.; Frere, J. M.; Ghuysen, J. M.; Joris, B.; Forsman, M.; Levesque, R. C.; Tiraby, G.; Waley, S. G. *Biochem. J.* **1991**, *276* (Pt 1), 269–270.

(14) Oefner, C.; D'Arcy, A.; Daly, J. J.; Gubernator, K.; Charnas, R. L.; Heinze, I.; Hubschwerlen, C.; Winkler, F. K. *Nature* **1990**, *343*, 284–288.

(15) Strynadka, N. C. J.; Adachi, H.; Jensen, S. E.; Johns, K.; Sielecki, A.; Betzel, C.; Sutoh, K.; James, M. N. G. *Nature* **1992**, *359*, 700–705.

(16) Guillaume, G.; Vanhove, M.; Lamotte-Brasseur, J.; Ledent, P.; Jamin, M.; Joris, B.; Frere, J. M. *J. Biol. Chem.* **1997**, *272*, 5438–5444.

(17) Hermann, J. C.; Ridder, L.; Höltje, H. D.; Mulholland, A. J. *Org. Biomol. Chem.* **2006**, *4*, 206–210.

(18) Matagne, A.; Lamotte-Brasseur, J.; Frere, J. M. *Biochem. J.* **1998**, *330* (Pt 2), 581–598.

(19) Massova, I.; Kollman, P. A. *J. Comput. Chem.* **2002**, *23*, 1559–1576.

(20) Diaz, N.; Sordo, T. L.; Merz Jr, K. M.; Suarez, D. *J. Am. Chem. Soc.* **2003**, *125*, 672–684.

(21) Atanasov, B. P.; Mustafi, D.; Makinen, M. W. *Proc. Natl. Acad. Sci. U.S.A.* **2000**, *97*, 3160–3165.

(22) Ishiguro, M.; Imajo, S. *J. Med. Chem.* **1996**, *39*, 2207–2218.

(23) Swaren, P.; Maveyraud, L.; Guillet, V.; Masson, J. M.; Mourey, L.; Samama, J. P. *Structure* **1995**, *3*, 603–613.

(24) Gibson, R. M.; Christensen, H.; Waley, S. G. *Biochem. J.* **1990**, *272*, 613–619.

(25) Lamotte-Brasseur, J.; Dive, G.; Dideberg, O.; Charlier, P.; Frere, J. M.; Ghuysen, J. M. *Biochem. J.* **1991**, *279* (Pt 1), 213–221.

(26) Meroueh, S. O.; Fisher, J. F.; Schlegel, H. B.; Mobashery, S. *J. Am. Chem. Soc.* **2005**, *127*, 15397–15407.

(27) Lodola, A.; Mor, M.; Hermann, J. C.; Tarzia, G.; Piomelli, D.; Mulholland, A. J. *Chem. Commun. (Camb.)* **2005**, 4399–4401.

(28) Diaz, N.; Suarez, D.; Sordo, T. L.; Merz, K. M. *J. Phys. Chem. B* **2001**, *105*, 11302–11313.

(29) Escobar, W. A.; Tan, A. K.; Fink, A. L. *Biochemistry* **1991**, *30*, 10783–10787.

(30) Adachi, H.; Ohta, T.; Matsuzawa, H. *J. Biol. Chem.* **1991**, *266*, 3186–3191.

(31) Lietz, E. J.; Truher, H.; Kahn, D.; Hokenson, M. J.; Fink, A. L. *Biochemistry* **2000**, *39*, 4971–4981.

(32) Lamotte-Brasseur, J.; Lounnas, V.; Raquet, X.; Wade, R. C. *Protein Sci.* **1999**, *8*, 404–409.

(33) Raquet, X.; Lounnas, V.; Lamotte-Brasseur, J.; Frere, J. M.; Wade, R. C. *Biophys. J.* **1997**, *73*, 2416–2426.

(34) Damblon, C.; Raquet, X.; Lian, L. Y.; Lamotte-Brasseur, J.; Fonze, E.; Charlier, P.; Roberts, G. C.; Frere, J. M. *Proc. Natl. Acad. Sci. U.S.A.* **1996**, *93*, 1747–1752.

(35) Minasov, G.; Wang, X.; Shoichet, B. K. *J. Am. Chem. Soc.* **2002**, *124*, 5333–5340.

(36) Nukaga, M.; Mayama, K.; Hujer, A. M.; Bonomo, R. A.; Knox, J. R. *J. Mol. Biol.* **2003**, *328*, 289–301.

(37) Hermann, J. C.; Ridder, L.; Mulholland, A. J.; Höltje, H. D. *J. Am. Chem. Soc.* **2003**, *125*, 9590–9591.

(38) Hermann, J. C.; Hensen, C.; Ridder, L.; Mulholland, A. J.; Höltje, H. D. *J. Am. Chem. Soc.* **2005**, *127*, 4454–4465.

(39) Delmas, J.; Chen, Y.; Prati, F.; Robin, F.; Shoichet, B. K.; Bonnet, R. *J. Mol. Biol.* **2008**, *375*, 192–201.

(40) Chen, Y.; Bonnet, R.; Shoichet, B. K. *J. Am. Chem. Soc.* **2007**, *129*, 5378–5380.

(41) Chen, Y.; Shoichet, B.; Bonnet, R. *J. Am. Chem. Soc.* **2005**, *127*, 5423–5434.

(42) Field, M. J.; Bash, P. A.; Karplus, M. *J. Comput. Chem.* **1990**, *11*, 700–733.

(43) Dewar, M. J. S.; Zoebisch, E. G.; Healy, E. F.; Stewart, J. J. P. *J. Am. Chem. Soc.* **1985**, *107*, 3902–3909.

(44) Hermann, J. C. *Thesis*; Cuvillier: Goettingen, 2004.

(45) Lewars, E. *In Computational Chemistry*; Kluwer Academic Publishers: Dordrecht, The Netherlands, 2003; pp 339−382.

(46) Claeyssens, F.; Harvey, J. N.; Manby, F. R.; Mata, R. A.; Mulholland, A. J.; Ranaghan, K. E.; Schütz, M.; Thiel, S.; Thiel, W.; Werner, H.-J. *Angew. Chem., Int. Ed.* **2006**, *45*, 6856–6859.

(47) Chen, C. C.; Smith, T. J.; Kapadia, G.; Wasch, S.; Zawadzke, L. E.; Coulson, A.; Herzberg, O. *Biochemistry* **1996**, *35*, 12251–12258.

(48) Harvey, J. N. *Faraday Discuss.* **2004**, *127*, 165–177.

(49) Claeyssens, F.; Ranaghan, K. E.; Manby, F. R.; Harvey, J. N.; Mulholland, A. J. *Chem. Commun.* **2005**, 5068–5070.

(50) Jaguar, Version 6.0, Schrödinger, LLC, New York, 2005.

(51) Ren, P.; Ponder, J. W. *J. Phys. Chem. B* **2003**, *107*, 5933–5947.

(52) Tinker-Software Tools for Molecular Design (http://dasher.wustl.edu/tinker; accessed 15/09/09).

(53) MacKerell, A. D.; Bashford, D.; Bellott, M.; Dunbrack, R. L.; Evanseck, J. D.; Field, M. J.; Fischer, S.; Gao, J.; Guo, H.; Ha, S.; Joseph-McCarthy, D.; Kuchnir, L.; Kuczera, K.; Lau, F. T. K.; Mattos, C.; Michnick, S.; Ngo, T.; Nguyen, D. T.; Prodhom, B.; Reiher, W. E.; Roux, B.; Schlenkrich, M.; Smith, J. C.; Stote, R.; Straub, J.; Watanabe, M.; Wiorkiewicz-Kuczera, J.; Yin, D.; Karplus, M. *J. Phys. Chem. B* **1998**, *102*, 3586–3616.

(54) Mulholland, A. J. *Biochem. Soc. Trans.* **2008**, *36*, 22–26.

(55) Zhao, Y.; Gonzalez-Garcia, N.; Truhlar, D. G. *J. Phys. Chem. A* **2005**, *109*, 2012–2018.

(56) Werner, H.-J.; Knowles, P. J.; Lindh, R.; Manby, F. R.; Schütz, M.; Celani, P.; Korona, T.; Rauhut, G.; Amos, R. D.; Bernhardsson, A.; Berning, A.; Cooper, D. L.; Deegan, M. J. O.; Dobbyn, A. J.; Eckert, F.; Hampel, C.; Hetzer, G.; Lloyd, A. W.; McNicholas, S. J.; Meyer, W.; Mura, M. E.; Nicklass, A.; Palmieri, P.; Pitzer, R.; Schumann, U.; Stoll, H.; Stone, A. J.; Tarroni, R.; Thorsteinsson, T. Molpro, 2006.1 ed. Molpro: Cardiff, U.K., 2006 (http://www.molpro.net/; accessed September 25, 2009).

(57) Grimme, S. *J. Chem. Phys.* **2003**, *118*, 9095–9102.

(58) Berman, H. M.; Westbrook, J.; Feng, Z.; Gilliland, G.; Bhat, T. N.; Weissig, H.; Shindyalov, I. N.; Bourne, P. E. *Nucleic Acids Res.* **2000**, *28*, 235–242.

(59) Warshel, A. *Annu. Rev. Biophys. Biomol. Struct.* **2003**, *32*, 425–443.

(60) Reuter, N.; Dejaegere, A.; Maigret, B.; Karplus, M. *J. Phys. Chem. A* **2000**, *104*, 1720–1735.

(61) Lodola, A.; Mor, M.; Zurek, J.; Tarzia, G.; Piomelli, D.; Harvey, J. N.; Mulholland, A. J. *Biophys. J.: Biophys. Lett.* **2007**, *92*, L20–l23.

(62) van der Kamp, M. W.; Perruccio, F.; Mulholland, A. J. *Chem. Commun.* **2008**, 1874–1876.

(63) van der Kamp, M. W.; Mulholland, A. J. *Nat. Prod. Rep.* **2008**, *25*, 1001–1014.

(64) Lyne, P. D.; Mulholland, A. J.; Richards, W. G. *J. Am. Chem. Soc.* **1995**, *117*, 11345–11350.

(65) Mulholland, A. J.; Richards, W. G. *Proteins: Struct., Funct. Genet.* **1997**, *27*, 9–25.

(66) Ridder, L.; Mulholland, A. J.; Rietjens, I. M. C. M.; Vervoort, J. *J. Am. Chem. Soc.* **2000**, *122*, 8728–8738.

(67) Ranaghan, K. E.; Masgrau, L.; Scrutton, N. S.; Sutcliffe, M. J.; Mulholland, A. J. *ChemPhysChem* **2007**, *8*, 1816–1835.

(68) Ridder, L.; Harvey, J. N.; Rietjens, I. M. C. M.; Vervoort, J.; Mulholland, A. J. *J. Phys. Chem. B* **2003**, *107*, 2118–2126.

(69) Garcia-Viloca, M.; Gao, J.; Karplus, M.; Truhlar, D. G. *Science* **2004**, *303*, 186–95.

(70) Fisher, J.; Belasco, J. G.; Khosla, S. *Biochemistry* **1980**, *19*, 2895–2901.

(71) Dalbadie-McFarland, G.; Neitzel, J. J.; Richards, J. H. *Biochemistry* **1986**, *25*, 332–338.

(72) Page, M. I. *Curr. Pharm. Des.* **1999**, *5*, 895–913.

(73) Kästner, J.; Senn, H. M.; Thiel, S.; Otte, N.; Thiel, W. *J. Chem. Theory Comput.* **2006**, *2*, 452–461.

(74) Masgrau, L.; Roujeinikova, A.; Johannissen, L. O.; Hothi, P.; Basran, J.; Ranaghan, K. E.; Mulholland, A. J.; Sutcliffe, M. J.; Scrutton, N. S.; Leys, D. *Science* **2006**, *312*, 237–241.

(75) Garcia-Viloca, M.; Gao, J.; Karplus, M.; Truhlar, D. G. *Science* **2004**, *303*, 186–195.

(76) Meyer, M. P.; Tomchick, D. R.; Klinman, J. P. *Proc. Natl. Acad. Sci. U.S.A.* **2008**, *105*, 1146–1151.

(77) Olsson, M. H. M.; Siegbahn, P. E. M.; Warshel, A. *J. Biol. Inorg. Chem.* **2004**, *9*, 96–99.
(78) Ranaghan, K. E.; Ridder, L.; Szefczyk, B.; Sokalski, W. A.; Hermann, J. C.; Mulholland, A. J. *Mol. Phys.* **2003**, *101*, 2695–2714.
(79) Lozynski, M.; Rusinska-Roszak, D.; Mack, H. G. *J. Phys. Chem. A* **1998**, *102*, 2899–2903.
(80) Dkhissi, A.; Adamowicz, L.; Maes, G. *J. Phys. Chem. A* **2000**, *104*, 2112–2119.
(81) Prabhakar, R.; Blomberg, M. R. A.; Siegbahn, P. E. M. *Theor. Chem. Acc.* **2000**, *104*, 461–470.
(82) Zheng, J.; Zhao, Y.; Truhlar, D. G. *J. Chem. Theory Comput.* **2007**, *3*, 569–582.
(83) Smith, C. A.; Caccamo, M.; Kantardjieff, K. A.; Vakulenko, S. *Acta Crystallogr., Sect. D Biol. Crystallogr.* **2007**, *63*, 982–992.
(84) Stackhouse, J.; Nambiar, K. P.; Burbaum, J.; Stauffer, D. M.; Benner, S. A. *J. Am. Chem. Soc.* **1985**, *107*, 2757–2763.
(85) Albery, W. J.; Knowles, J. R. *Angew. Chem., Int. Ed. Engl.* **1977**, *16*, 285–293.
(86) Oliva, C.; Rodríguez, A.; González, M.; Yang, W. *Biochemistry* **2007**, *66*, 444–455.
(87) Bakowies, D.; Kollman, P. A. *J. Am. Chem. Soc.* **1999**, *121*, 5712–5726.
(88) Blumberger, J.; Ensing, B.; Klein, M. L. *Angew. Chem. Int. Ed.* **2006**, *45*, 2893–2897.
(89) Blumberger, J.; Klein, M. L. *Chem. Phys. Lett.* **2006**, *422*, 210–217.
(90) Strajbl, M.; Florian, J.; Warshel, A. *J. Am. Chem. Soc.* **2000**, *122*, 5434–5366.
(91) Warshel, A.; Åqvist, J.; Creighton, S. *Proc. Natl. Acad. Sci. U.S.A.* **1989**, *86*, 5820–5824.
(92) Dal Peraro, M.; Llarrull, L. I.; Röthlisberger, U.; Vila, A. J.; Carloni, P. *J. Am. Chem. Soc.* **2004**, *126*, 12661–12668.
(93) Park, H.; Brothers, E. N.; Merz, K. M., Jr. *J. Am. Chem. Soc.* **2005**, *127*, 4232–4241.
(94) Xu, D.; Guo, H. *J. Am. Chem. Soc.* **2009**, *131*, 9780–9788.
(95) Szeto, M. W. Y.; Mujika, J. I.; Zurek, J.; Mulholland, A. J.; Harvey, J. N. *J. Mol. Struct.: THEOCHEM* **2009**, *898*, 106–114.
(96) Szefczyk, B.; Claeyssens, F.; Mulholland, A. J.; Sokalski, W. A. *Int. J. Quantum Chem.* **2007**, *107*, 2274–2285.
(97) Harvey, J. N.; Aggarwal, V. K.; Bathelt, C. M.; Carreón-Macedo, J.-L.; Gallagher, T.; Holzmann, N.; Mulholland, A. J.; Robiette, R. *J. Phys. Org. Chem.* **2006**, *19*, 608–615.
(98) Altun, A.; Shaik, S.; Thiel, W. *J. Comput. Chem.* **2006**, *27*, 1324–1337.
(99) Castillo, R.; Silla, E.; Tunon, I. *J. Am. Chem. Soc.* **2002**, *124*, 1809–1816.
(100) Bowman, A. L.; Ridder, L.; Rietjens, I. M. C. M.; Vervoort, J.; Mulholland, A. J. *Biochemistry* **2007**, *46*, 6353–6363.
(101) Kamerlin, S. C. L.; Haranczyk, M.; Warshel, A. *J. Phys. Chem. B* **2009**, *113*, 1253–1272.
(102) Woods, C. J.; Manby, F. R.; Mulholland, A. J. *J. Chem. Phys.* **2008**, *128*, 014109.
(103) Mulholland, A. J. *Chem. Central J.* **2007**, *1*, 19 (http://journal.chemistrycentral.com/content/1/1/19; accessed September 25, 2009).
(104) Senthilkumar, K.; Mujika, J. I.; Ranaghan, K. E.; Manby, F. R.; Mulholland, A. J.; Harvey, J. N. *J. R. Soc. Interface* **2008**, *5*, S207–216.
(105) Lietz, E. J.; Truher, H.; Kahn, D.; Hokenson, M. J.; Fink, A. L. *Biochemistry* **2000**, *39*, 4971–4981.

JP9037254